



First principle investigation of electronic structure and optical behaviors of 2-amino-4-fluorododec-4-encarboic acid



A.H. Reshak^{a,b}, Saleem Ayaz Khan^{a,*}

^a New Technologies—Research Center, University of West Bohemia, Univerzitni 8, 306 14 Pilsen, Czech Republic

^b Center of Excellence Geopolymer and Green Technology, School of Material Engineering, University Malaysia Perlis, 01007 Kangar, Perlis, Malaysia

ARTICLE INFO

Keywords:

Electronic structure
Charge density
Optical properties

ABSTRACT

The electronic structure and dispersion of optical susceptibilities of 2-amino-4-fluorododec-4-encarboic acid were calculated using all-electron full potential linear augmented plane wave method based on density functional theory. Perdew–Burke–Ernzerhof generalized gradient approximation (PBE-GGA) and Engel Vosko generalized gradient approximation (EV-GGA) were used to solve the exchange correlation functional. The EV-GGA scheme was selected to obtain better band gap value (4.91 eV) as compared to GGA-PBE (4.75 eV). The valence electron charge density plots show foremost covalent nature of the bonds. The C–C bond is pure covalent bond while C–H, C–F, C–O, N–H and C–N configuration show dominant covalent bond with small percentage of ionicity. The calculated spectral peaks in $\epsilon_2(\omega)$ show electron transition between the occupied and unoccupied bands. The calculated absorption coefficient $I(\omega)$ and reflectivity spectra $R(\omega)$ of 2-amino-4-fluorododec-4-encarboic acid show response to electromagnetic radiation in extreme ultraviolet region (UV-C). The dispersion of calculated second order dielectric tensor components $\epsilon_2(\omega)$, $\epsilon_1(\omega)$, $I(\omega)$ and $L(\omega)$ show considerable anisotropy.

© 2014 Elsevier Ltd. All rights reserved.

1. Introduction

Recently fluoro-organic chemistry got considerable attention because of astonishing evolution and a marked impact in designing and synthesis of large scale of biologically active molecules like amines, amino-acids, peptides along with other natural products [1]. The importance of the naturally occurring amino acids can't be ignored because of its essential role in living system [1].

Amino acids are the building block of proteins and peptides. Its different types have fascinating characteristics. Amino acids have a multiplicity of structural parts, which expose unusual solubility and polarities [2]. The synthetic fluorine

containing amino acids have always been an interesting topic for scientists in order to modify the physiological processes [3–9]. The organic molecules modified by fluorine, tune the properties of molecules for special applications which is widely used for development of pharmaceutical research (diagnostics of brain tumors and nuclear medicine techniques), for bioactivity in a large range of agrochemical products such as pesticides contains fungicides, herbicides and insecticides. It also play a vital role in soft materials chemistry for example self assembling monolayer, photoresist polymers, positron emission tomography and liquid crystals [4,10–21]. Liquid crystal technology is very important and play major role in many fields of science and engineering especially in device technology such as liquid crystal displays, liquid crystal thermometers, optical imaging and polymer dispersed liquid crystals [22]. Liquid crystals are used for nondestructive under stress mechanical test of materials. This method can also be

* Corresponding author. Tel.: +420 777 083 956.
E-mail address: sayaz_usb@yahoo.com (S.A. Khan).

applied to visualize the radio frequency waves (RFW) in waveguides and some medical purpose like transient pressure transmitted [22]. The constituent molecules of the liquid crystals are the fluid segment, which are appropriately scattered to be rated as a liquid, and possessing the flow features, preserve the actual type of liquid crystal phase, depending on the fluctuating degrees of ordering. As is known that these crystals (liquid) are anisotropic fluids so their flow and molecular combination presents good optical, dielectric, and viscoelastic properties [23]. Generally the liquid crystals show anisotropy which elucidates different behaviors from molecule to molecules depends on the direction. Weak electric field changes the orientation of the liquid crystals and makes it suitable for display application [23].

Amino acids from the chiral pool looked to be perfect precursor for ionic liquid crystals due to their good accessibility and small cost [24]. Many examples, which use amino acids as a reagent, are from task-specific organic liquid crystals, [25] whereas amino acid can be either cation [26] or anion [27].

The amino acids are good contestant for liquid crystal applications because of its low cost and easily availability; therefore; it is necessary to highlight its optoelectronic properties. We should emphasize that the introduction of halogen into the organic molecule has an effective way to improve some properties such as stability, rigidity and optical properties due to the high strengths of the C–X bonds [28]. In this work we are interested to evaluate the electronic structure, valence electron charge density along with the dispersions of the optical properties of 2-amino-4-fluorododec-4-encarboic acid using all-electron full potential linear augmented plane wave (FPLAPW) method which has been confirmed to be one of the most precise methods for calculating the electronic structure and optical properties within in DFT [29,30].

2. Crystal structure and computational details

The chemical formula of 2-amino-4-fluorododec-4-encarboic acid is $C_{12}H_{22}FNO_2$. It is stable in monoclinic phase having space group $P2_1/c$ with four formula units per unit cell. The lattice parameters are $a=28.081 \text{ \AA}$, $b=4.874 \text{ \AA}$, $c=9.694 \text{ \AA}$ with $\beta=93.21^\circ$. The crystallographic data for 2-amino-4-fluorododec-4-encarboic acid have been taken from Cambridge Crystallographic data Center (CCDC) having deposition number 252332. The molecular structure and unit cell of 2-amino-4-fluorododec-4-encarboic acid are shown in Fig. 1a and b.

In this work we have calculated the electronic band structure, density of states (DOS), electronic charge density and optical susceptibilities of 2-amino-4-fluorododec-4-encarboic acid. The calculations were performed using all-electron full potential linear augmented plane wave (FPLAPW) method within WIEN2k code [31–33]. The exchange correlation potential (V_{xc}) was solved by Perdew–Burke–Ernzerhof generalized gradient approximation (PBE – GGA) [34] and Engel Vosko generalized gradient approximation (EV – GGA) [35]. In order to converge the energy eigenvalues, the wave function in the interstitial regions were expended in plane waves with cutoff $R_{MT}K_{max}=7.0$. The R_{MT} stand for the muffin-tin (MT) sphere radius and K_{max} shows the magnitude

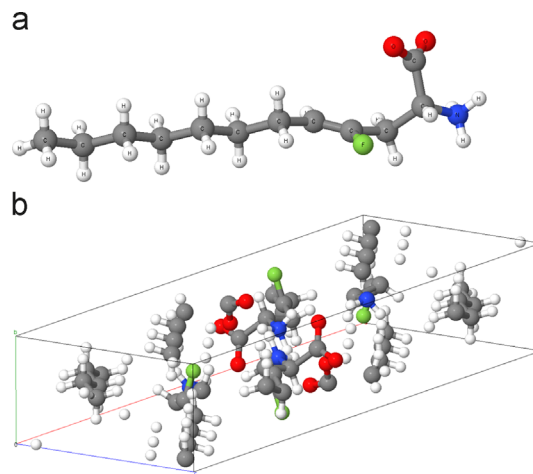


Fig. 1. (a) Optimize molecular structure of 2-amino-4-fluorododec-4-encarboic acid, (b) unit cell of 2-amino-4-fluorododec-4-encarboic acid.

of largest K vector in expansion of plane wave. The selected R_{MT} are 1.03, 1.06, 0.53, 0.98 and 1.16 a.u. for C, O, H, N and F atom, respectively. The wave function inside the sphere was expended up to $l_{max}=10$ whereas the Fourier expansion of the charge density was up to $G_{max}=26 \text{ (a.u.)}^{-1}$. We have optimized the structure by minimizing of forces acting on the atoms. The convergence of the self-consistent calculation was done when the difference in total energy of the crystal did not exceed 10^{-2} mRyd in successive steps. The self-consistencies were obtained by 126k points in irreducible Brillouin zones (IBZ).

3. Result and discussions

3.1. Band structure and density of states

The calculating band structure provides the information about the electronic structure and optical response of the material and its basis are directly connected to density of states [36,37]. We have calculated electronic band structure of 2-amino-4-fluorododec-4-encarboic acid along high symmetry lines of the Brillouin zone (Z–D– Γ –Y–Z) using PBE-GGA and EV-GGA as shown in Fig. 2. Usually PBE-GGA leads to underestimate the band gap value. The PBE-GGA has simple form which is not adequately flexible to accurate calculation of exchange-correlation energy and its charge derivative. Generally EV-GGA acquired by optimizing the exchange-correlation potential V_{xc} as an alternative of the corresponding energy E_{xc} . This approach exhibit better band splitting and structural properties that depend on the precision of the exchange–correlation potential [38–40]. The electronic band structure of 2-amino-4-fluorododec-4-encarboic acid calculated by PBE-GGA is shown in Fig. 2a. The dispersion of the electronic band structure visualize that the valence band maximum (VBM) and the conduction minimum (CBM) are located at Z point of the BZ results the a direct band gap semiconductor of about 4.75 eV. As one move from PBE-GGA to EV-GGA the conduction band minimum shift towards higher energies resulting in increase the band gap value to be 4.91 eV as shown in Fig. 2b. As EV-GGA scheme show better band splitting and as a consequence better band gap

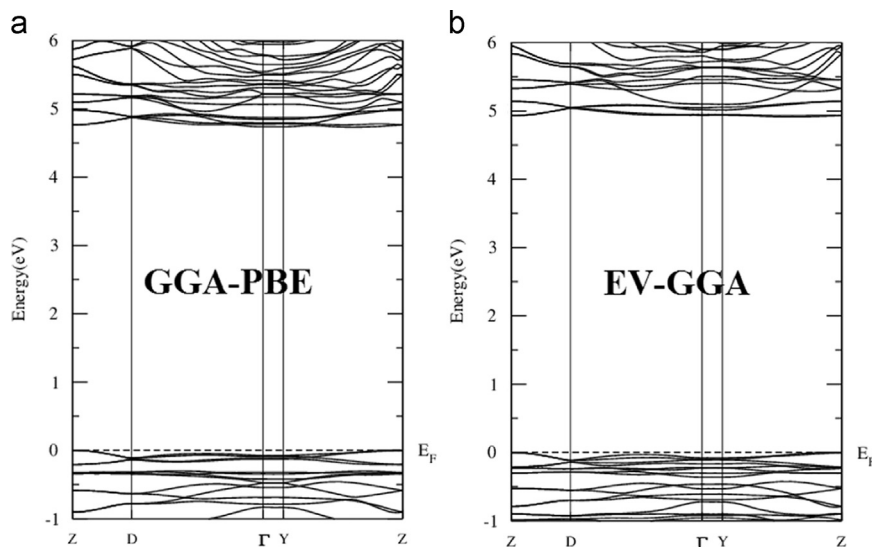


Fig. 2. Calculated band structure of 2-amino-4-fluorododec-4-encarboic acid.

therefore this scheme was selected for further explanation of density of states, charge density and optical properties. The calculated bands are less dispersed (much flatter) which results in small mobility of the charge carrier (holes and electrons).

The calculated total density of states (TDOS) and partial density of states (PDOS) of 2-amino-4-fluorododec-4-encarboic acid are shown in Fig. 3a and b. The TDOS assign the electronic band structure of the material and show density of states in unit cell at different energy level. Further, PDOS show the contribution of orbital in bands formations. From -9.0 eV to -2.0 eV, the bands are formed by C-s/p, F-s/p, O-s/p, H-s and N-s/p states. The F-s state is dominant in this range with maximum density of 0.7 states/eV. The next foremost states are C-p and O-p which show the value of 0.3 states/eV and 0.25 states/eV while C-s and F-p states play intermediate role (0.16 states/eV and 0.15 states/eV). Other states such as N-s/p and H-s shows small contribution in this range. From -2.0 eV to Fermi level the O-p state show dominance with density value of 0.25 states/eV which play main role in valence band formation. The contribution of F-s state reduced to 0.1 states/eV, while H-s and C-s/p states show negligible contribution in this range. The conduction band around 4.8 eV is primarily fashioned by C-p (0.8 states/eV) and O-p states (0.3 states/eV). The other states (N-s/p, O-s, F-s/p, and H-s) show small contribution. In the energy range between 6.0 eV and 20.5 eV, the bands are formed by combination of C-s/p, N-s/p, O-s/p, H-s, and F-s/p states. F-s state is predominant (0.2 states/eV) in this region.

There exists a strong hybridization among s and p states of C, N, H, F and O atoms resulting in a covalent nature of the bond, which can be observed from the electronic charge density contour.

3.2. Electronic charge density

The precise bonding nature of the compound can be estimated from the valence electron charge density plot [41,42]. We have calculated the electronic charge density

distribution for 2-amino-4-fluorododec-4-encarboic acid to visualize the bonding nature. Fig. 4a–c represents the electronic charge density contours in different crystallographic planes. The blue region in the contour plot shows maximum charge density region and the red color region exhibits zero charge according to the thermoscale attached to Fig. 4a–c.

Fig. 4a exhibits that there exists a strong covalent bond between C–C, C–H, C–F and C–O atoms and the electronic charge is concentrated around these atoms as indicated by blue color; whereas Fig. 4b shows a covalent bond between C–H and C–C atoms while F and N atoms exhibit strong ionic bonds and very weak covalent bonds with C atom. Fig. 4c shows a strong covalent bond between C–O, C–C, C–N, N–H atoms. In the present work we also calculated the ionicity of the compound in term of electronegativity difference between C–H (0.4), C–C (0.0), C–O (1.0), C–F (1.5), C–N (0.5) and N–H (0.9). Using Pauling empirical formula [43] and its selection rules, we calculated the bonding nature and percentage ionicity as shown in Table 1.

If the electronegativity difference is < 1.7 , it results small percentage of ionicity and strong covalent nature between the atoms. As the electronegativity difference decreases the covalent bond is going to be more dominant. It is clear from Table 1 and Fig. 4a–c that the overall bonding behavior of 2-amino-4-fluorododec-4-encarboic acid is covalent with small part of ionicity. The blue region in Fig. 4a–c exists due to delocalize electrons.

3.3. Optical properties

The energy band structure of solid is directly linked with the complex dielectric function $\epsilon(\omega)$ which establishes the overall band behavior. In the complex dielectric function $\epsilon(\omega) = \epsilon_1(\omega) + i\epsilon_2(\omega)$ the real part is correlated to electric polarizability of the material while the imaginary part show the absorption of energy and transition of electron to excited states [44–46]. The dispersions of dielectric function

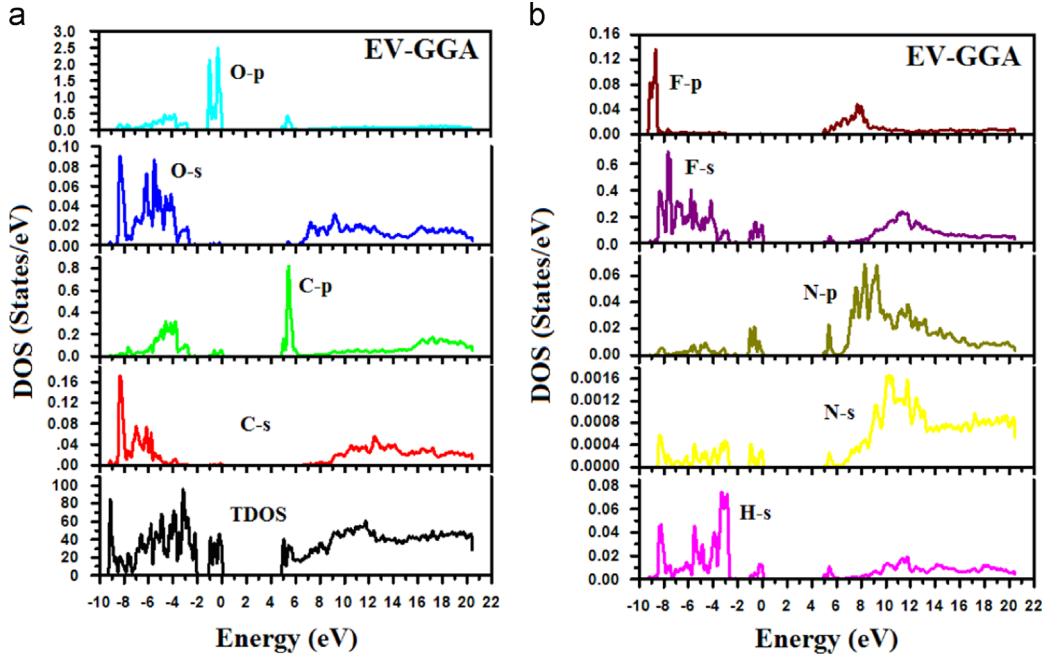


Fig. 3. Calculated total and partial density of states (states/eV unit cell) of 2-amino-4-fluorododec-4-encarboic acid.

include intra-band transition along with inter-band transitions. The intra-band transitions are significant only in case of metals and can be ignored for semiconducting materials. The correct energy eigenvalues in addition to electron wave functions are required for complete description of dielectric function $\epsilon(\omega)$ which is a natural output of calculated electronic band structure. The crystal structure symmetry of 2-amino-4-fluorododec-4-encarboic acid allows several nonzero second order dielectric tensor components. For simplicity we take only the three principal diagonals of dielectric tensor components. These are $\epsilon^{xx}(\omega)$, $\epsilon^{yy}(\omega)$ and $\epsilon^{zz}(\omega)$ along **a**, **b** and **c** crystallographic axes. The dielectric tensor components of $\epsilon_2(\omega)$ are obligatory for full detail of linear optical susceptibilities of the investigated compound. The required dielectric tensor components can be calculated using the expression given in Ref. [47].

$$\epsilon_2^{ij} = \frac{4\pi^2 e^2}{Vm^2\omega^2} \times \sum_{mn'\sigma} \langle kn\sigma | p_i | kn'\sigma \rangle \langle kn'\sigma | p_j | kn\sigma \rangle \times f_{kn} (1 - f_{kn'}) \delta(E_{kn'} - E_{kn} - \hbar\omega) \quad (1)$$

where m stands for mass and e for the charge of electron and ω represents the electromagnetic radiation (EM) striking the crystal of unit cell volume (V). In bracket notation p corresponds to the momentum operator, $|kn\sigma\rangle$ shows the crystal wave function with crystal momentum k and σ spin which correspond to the eigenvalue E_{kn} . The Fermi distribution function is represented by f_{kn} which makes sure the counting of transition between the occupied and unoccupied states and $\delta(E_{kn'} - E_{kn} - \hbar\omega)$ shows the condition for conservation of total energy.

The 2-amino-4-fluorododec-4-encarboic acid is a direct band gap ($Z \rightarrow Z$) semiconductor which shows high transparency up to 4.91 eV. When the energy of the electromagnetic radiation becomes greater than 4.91 eV it allows the absorption to begin as shown in Fig. 5a. The peaks in the

spectral structure of optical spectra elucidate electron transition between occupied and unoccupied bands. The first peak shows transition of electron from predominant F-s and O-p states around the Z point of BZ to C-p and O-p. The rest peaks show electron transitions from semi-core occupied bands to high energy unoccupied bands. The real part of dielectric function is calculated from imaginary part using Kramer-Kronig relation [48].

$$\epsilon_1(\omega) = 1 + \frac{2P}{\pi} \int_0^\infty \frac{\omega' \epsilon_2(\omega')}{\omega'^2 - \omega^2} d\omega' \quad (2)$$

where P represents the principal value of integral. Fig. 5b represents the calculated dispersion of real part of dielectric function $\epsilon_1(\omega)$. The three principal components $\epsilon_1^{xx}(\omega)$, $\epsilon_1^{yy}(\omega)$ and $\epsilon_1^{zz}(\omega)$ show isotropic behavior from 0.0 eV to 4.0 eV. There is a considerable anisotropy among these components from 4.0 eV to 12.0 eV. For higher energy range, the three components are isotropic as shown in Fig. 5b.

We have evaluated the other optical properties such as refractive indices $n(\omega)$, absorption coefficient $I(\omega)$, reflectivity $R(\omega)$, and energy loss function $L(\omega)$ by using the calculated spectra of $\epsilon_1(\omega)$ and $\epsilon_2(\omega)$ as shown in Fig. 5(c–f). The calculated static values of nonzero tensor components of the real part of dielectric tensor components and the refractive indices are shown in Table 2. It is obvious that $\epsilon_1(0)$ is directly related to $n(0)$ by the relation $n(0) = \sqrt{\epsilon_1(0)}$.

When the energy of incident radiations is gradually increased the spectral components of refractive indices of $n^{xx}(\omega)$ and $n^{zz}(\omega)$ reaches to its maximum value of 1.93 and 1.74 around 5.0 eV. The spectral peak of $n^{yy}(\omega)$ shows its maximum value (1.88) around 7.8 eV. The refractive indices of the investigated compound are represented in Fig. 4c. It is clear that $n^{xx}(\omega)$, $n^{yy}(\omega)$ and $n^{zz}(\omega)$ show isotropy from 0.0 eV to 4.0 eV and from 12.5 eV to 13.5 eV. There exists a considerable anisotropy between 4.0 eV and 12.5 eV.

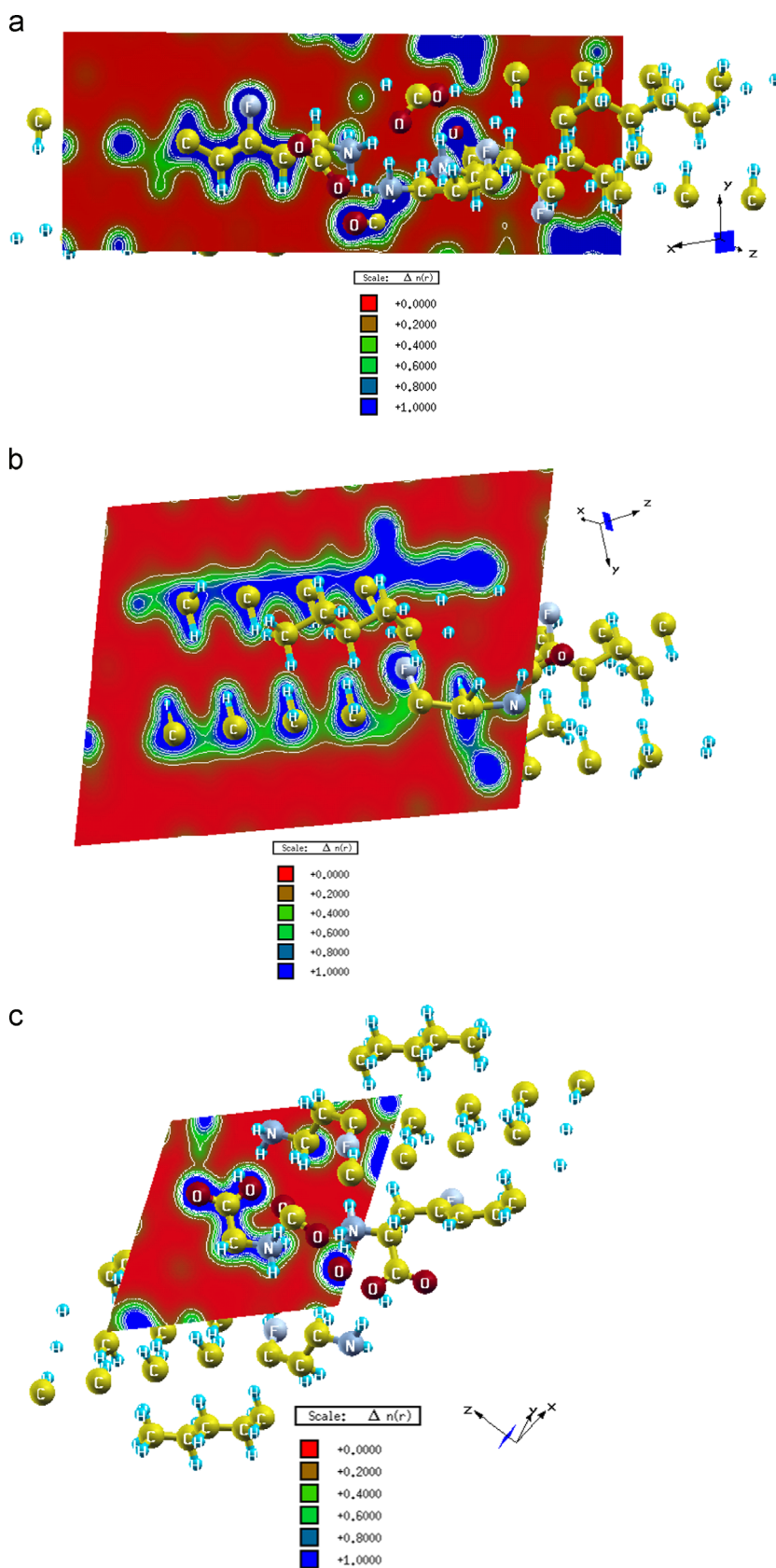


Fig. 4. Electronic charge density contour of 2-amino-4-fluorododec-4-encarboic acid.

Table 1

Calculated ionicity (%) between bonds of 2-amino-4-fluorododec-4-encarboic acid.

Bond	X_A-X_B	Bond nature	Polarity	% Ionicity
C–C	0.00	Covalent	Non polar	0.00
C–N	0.50	"	"	08.87
N–H	0.90	"	"	17.23
C–H	0.40	"	"	06.96
C–O	1.00	"	Polar	19.50
C–F	1.50	"	"	31.87

Table 2

Calculated static optical constants of 2-amino-4-fluoro-dodec-4-encarboic acid.

Static constant	
$\epsilon_1^{xx}(0)$	1.887
$\epsilon_1^{yy}(0)$	1.928
$\epsilon_1^{zz}(0)$	1.926
$n^{xx}(0)$	1.374
$n^{yy}(0)$	1.388
$n^{zz}(0)$	1.387

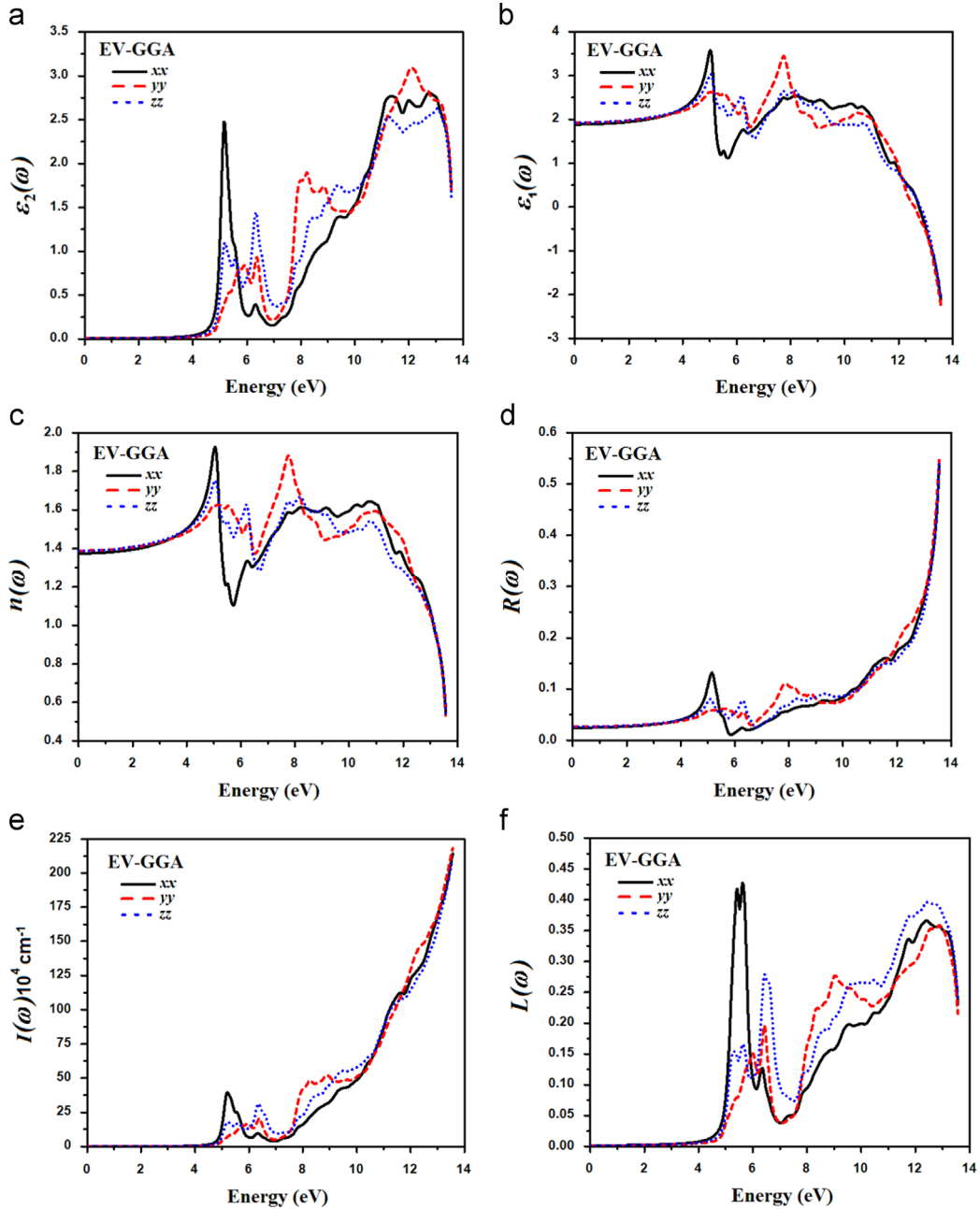


Fig. 5. (a) Calculated $\epsilon_2^{xx}(\omega)$, $\epsilon_2^{yy}(\omega)$ and $\epsilon_2^{zz}(\omega)$, (b) calculated $\epsilon_1^{xx}(\omega)$, $\epsilon_1^{yy}(\omega)$ and $\epsilon_1^{zz}(\omega)$, (c) calculated $n^{xx}(\omega)$, $n^{yy}(\omega)$ and $n^{zz}(\omega)$, (d) calculated $R^{xx}(\omega)$, $R^{yy}(\omega)$ and $R^{zz}(\omega)$, (e) calculated $I^{xx}(\omega)$, $I^{yy}(\omega)$ and $I^{zz}(\omega)$, (f) calculated $L^{xx}(\omega)$, $L^{yy}(\omega)$ and $L^{zz}(\omega)$.

The interaction of photons with electrons is probably related to bonding nature of the elements in 2-amino-4-fluorododec-4-encarboic acid. Covalent nature of C–C, C–N, C–H, C–O, C–F, C–N and N–H shows greater photon–electron interaction, results increase in $n(\omega)$.

The three nonzero components of $R(\omega)$ are represented in Fig. 4d. At around 5.0 eV, $R^{xx}(\omega)$ show 13% reflection while $R^{yy}(\omega)$ and $R^{zz}(\omega)$ show small value of reflectivity (2.5% and 5.0%). At around 7.8 eV, $R^{yy}(\omega)$ increased to 10.0%. Around 13.5 eV, the three spectral components of reflectivity reached the maximum value where the reflection is about 55.0% in the overall spectrum.

The absorption coefficient $I(\omega)$ of 2-amino-4-fluorododec-4-encarboic acid, related to the band gap and shows short cut-off response in UV region, has increased from 4.91 eV. $I^{xx}(\omega)$ represents the first peak of about $38.0 \times 10^4 \text{ cm}^{-1}$ around 5.1 eV (Fig. 4e), whereas both $I^{yy}(\omega)$ and $I^{zz}(\omega)$ exhibit the first peak of about $20.0 \times 10^4 \text{ cm}^{-1}$ and $30.0 \times 10^4 \text{ cm}^{-1}$ at 6.4 eV. The three components $I^{xx}(\omega)$, $I^{yy}(\omega)$ and $I^{zz}(\omega)$ reach its minimum value at around 13.0 eV. As one moves toward higher energy, there is a steep increase in the spectral components of the absorption coefficient which shows maximum value of $215.0 \times 10^4 \text{ cm}^{-1}$ at around 13.6 eV. The three spectral components show considerable anisotropy in energy range (5.0–10.5) eV and (11.75–13.0) eV while the rest of range show isotropy. The energy loss function (Fig. 4f) $L(\omega)$ expresses the energy loss of fast electron that moving in the crystal. The sharp peaks in $L(\omega)$ at 5.6 eV and 6.4 eV are because of plasma oscillation [49]. The three spectral components show isotropy in lower (up to 5.0 eV) and higher energy range (around 13.5 eV). There is considerable anisotropy among $L^{xx}(\omega)$, $L^{yy}(\omega)$ and $L^{zz}(\omega)$ from 5.0 eV to 13.0 eV.

4. Conclusion

In present work the electronic band structure, valence electron charge density and optical properties of 2-amino-4-fluorododec-4-encarboic acid were calculated. The all-electron full potential linear augmented plane wave (FP-LAPW) method as implemented in WIEN2k code within the framework of DFT was used. The PBE-GGA and EV-GGA schemes were used to solve the exchange correlation potential. The electronic band structure calculations make favor of EV-GGA scheme for better band splitting which clarified that 2-amino-4-fluorododec-4-encarboic acid possess a wide band gap (4.91 eV). This scheme was preferred for further justification of total and partial density of states, valence electron charge density and optical properties of 2-amino-4-fluorododec-4-encarboic acid. The calculated valence electron charge density contour plots show dominant covalent and weak ionic nature of bonds. The percentage ionicity between C–O, C–H, C–F, N–H and C–N bonds was calculated using Pauling selection rules. The complex dielectric function, absorption coefficient, refractive index, reflectivity and energy loss function were calculated and discussed with full details. The three principal tensor components of complex dielectric function, and its derivatives show considerable anisotropy.

Acknowledgment

The result was developed within the CENTEM project, reg. no. CZ.1.05/2.1.00/03.0088, co-funded by the ERDF as part of the Ministry of Education, Youth and Sports OP RDI program. Computational resources were provided by MetaCentrum (LM2010005) and CERIT-SC (CZ.1.05/3.2.00/08.0144) infrastructures.

References

- [1] D.N.T. Kumar, Nooki Mehdi, Fenglin Huang, Min Zhang, Qufu Wei, *Int. J. Eng. Res. Appl.* 2 (2012) 077–086.
- [2] V.P. Kukhar, H.R. Hudson, in: V.P. Kukhar (Ed.), *Aminophosphonic and Aminophosphinic Acids*, J. Wiley and Sons, 2000.
- [3] R. Smits, C.D. Cadicamo, K. Burger, B. Koksche, *Chem. Soc. Rev.* 37 (2008) 1727–1739.
- [4] R. Filler, R. Saha, *Future Med. Chem.* 1 (2009) 777–791.
- [5] Kurt H. Piepenbrink, Oleg Y. Borbulevych, Ruth F. Sommese, John Clemens, Kathryn M. Armstrong, Clare Desmond, Priscilla Do, Brian M. Baker, *Biochem. J.* 423 (2009) 353–361.
- [6] M. Salwiczek, S. Samsonov, T. Vagt, E. Nyakatura, E. Fleige, J. Numata, M. T. Cölfen, M.T. Pisabarro, B. Koksche, *Chemistry* 15 (2009) 7628–7636.
- [7] N. Voloshchuk, J.K. Montclare, *Mol. Biosyst.* 6 (2010) 65–80.
- [8] M. Salwiczek, E.K. Nyakatura, Ulla I.M. Gerling, S. Ye, B. Koksche, *Chem. Soc. Rev.* 41 (2012) 2135–2171.
- [9] M. Duca, S.X. Chen, S.M. Hecht, *Methods* 44 (2008) 87–99.
- [10] B.K. Park, Neil R. Kitteringham, Paul M.O. Neill, *Annu. Rev. Pharmacol. Toxicol.* 41 (2001) 443–470.
- [11] D.A. Dougherty, *Curr. Opin. Chem. Biol.* 4 (2000) 645–652.
- [12] Gómez-Núñez Marta, Kurtis J. Haro, Tao Dao, Chau Deming, Won Annie, S. Zakhaleva Escobar-Alvarez, V. Korontsvit, T. Gin, David Y. Scheinberg, *PLoS One* 3 (2008) 3938.
- [13] H. Uchino, Y. Kanai, D.K. Kim, M.F. Wempe, A. Chairoungdua, E. Morimoto, M.W. Anders, H. Endou, *Mol. Pharmacol.* 61 (2002) 729–737.
- [14] N.C. Yoder, K. Kumar, *Chem. Soc. Rev.* 31 (2002) 335341.
- [15] (http://www.biology.arizona.edu/biochemistry/problem_sets/aa/aa.html#Essentialaa), 2011.
- [16] K. Yokota, M. Hagimori, N. Mizuyama, Y. Nishimura, H. Fujito, Y. Shigemitsu, Y. Tominaga, *Beilstein J. Org. Chem.* 8 (2012) 266–274.
- [17] Henry C. Brown, Charles R. Wetzel, *J. Org. Chem.* 30 (1965) 37243728.
- [18] M.P. Grinblat, I.V. Ikonitskii, N.Ye. Gordiyenko, M.M. Fomicheva, *Polym. Sci. U.S.S.R.* 21 (1980) 14341441.
- [19] K.J.L. Paciorek, J.H. Nakahara, R.H. Kratzer, *J. Fluorine Chem.* 30 (1985) 241250.
- [20] W.M.A. Grootaert, Robert E. Kolb, Klaus Hintzer, US PATENT Number: 6794457, Issue Date: Sep 21, 2004.
- [21] Peter Maienfisch, Roger G Hall, *CHIMIA Int. J. Chem.* 58 (2004) 93–99.
- [22] Denis Andrienko, International Max Planck Research School Modelling of Soft Matter, Bad Marienberg, 11–15 September, 2006, 2006.
- [23] M. Hird, *Chem. Soc. Rev.* 36 (2007) 2070–2095.
- [24] M. Mansueto, W. Frey, S. Laschat, *Chem. Eur. J.* 19 (2013) 16058–16065.
- [25] M. Li, D. Bwambok, S. Fakayode, I. Warner in (Ed. A. Berthod), Springer, Berlin, 2010, pp. 289–329.
- [26] S.-P. Luo, D.-Q. Xu, H.-D. Yue, L.-P. Wang, W.-L. Yang, Z.-Y. Xu, *Tetrahedron: Asymmetry* 17 (2006) 2028–2033.
- [27] S. Kasahara, E. Kamio, T. Ishigami, H. Matsuyama, *Chem. Commun.* 48 (2012) 6903–6905.
- [28] P.N. Gaponik, Y.V. Grigoriev, *AN Belarusi Izvestiya, Seriya Khim. Nauk* 1 (1992) 73–77.
- [29] S. Gao, *Comput. Phys. Commun.* 153 (2003) 190–198.
- [30] K. Schwarz, *J. Solid State Chem.* 176 (2003) 319–328.
- [31] P. Blaha, K. Schwartz, G.K.H. Madsen, D. Kvasnicka, J. Luitz, WIEN2K, An Augmented Plane Wave+Local Orbitals Program for Calculating Crystals Properties, Karlheinz Schwartz, Techn. Universitat, Wien, Austria, ISBN 3-9501031-1-2, 2001.
- [32] K.M. Wong, S.M. Alay-e-Abbas, A. Shaukat, Y. Fang, Y. Lei, *J. Appl. Phys.* 113 (2013) 014304.
- [33] K.M. Wong, S.M. Alay-e-Abbas, Y. Fang, A. Shaukat, Y. Lei, *J. Appl. Phys.* 114 (2013) 034901.

- [34] J.P. Perdew, K. Burke, M. Ernzerhof, *Phys. Rev. Lett* 77 (1996) 3865–3868.
- [35] E. Engel, S.H. Vosko, *Phys. Rev. B* 47 (1993) 13164.
- [36] S.A. Khan, A.H. Reshak, *Int. J. Electrochem. Sci.* 8 (2013) 9459–9473.
- [37] A.H. Reshak, S.A. Khan, S. Auluck, *RSC Adv* 4 (2014) 6957–6964.
- [38] Z. Charifi, H. Baaziz, A.H. Reshak, *Phys. Status Solidi B* 244 (2007) 3154.
- [39] A.H. Reshak, S.A. Khan, H. Kamarudin, *Jiri Bila, J. Alloys Compd.* 582 (2014) 6–11.
- [40] A.H. Reshak, S.A. Khan, *Comput. Mater. Sci.* 78 (2013) 91.
- [41] R. Hoffman, *Rev. Mod. Phys.* 60 (1988) 601–628.
- [42] C.D. Gellatt, A.R. Willaims Jr., V.L. Moruzzi, *Phys. Rev. B* 27 (1983) 2005–2013.
- [43] *Schlüsseltechnologien Key Technologies*, 41st IFF Springschool, 2010, pp A1.18.
- [44] A.H. Reshak, S.A. Khan, S. Auluck, *RSC Adv* 4 (2014) 11967–11974.
- [45] S.A. Khan, A.H. Reshak, *Comput. Mater. Sci.* 95 (2014) 328–336.
- [46] S.A. Khan, A.H. Reshak, *Polyhedron* 85 (2015) 962–970.
- [47] A. Delin, P. Ravindran, O. Eriksson, J.M. Wills, *Int. J. Quantum Chem.* 69 (1998) 349.
- [48] H. Tributsch, *Z. Naturforsch, A* 32A (1977) 972.
- [49] L. Marton, *Rev. Mod. Phys.* 28 (1956) 172.